Measuring and modelling overwash hydrodynamics on a barrier island

Matias, Ana; Carrasco, Ana Rita; Loureiro, Carlos; Andriolo, Umberto; Masselink, Gerd; Guerreiro, Martha; Pacheco, A; McCall, R.T.; Ferreira, Óscar; Plomaritis, Theocharis A.

Publication date
2017

Document Version
Final published version

Published in
Proceedings of Coastal Dynamics 2017

Citation (APA)
Matias, A., Carrasco, A. R., Loureiro, C., Andriolo, U., Masselink, G., Guerreiro, M., Pacheco, A., McCall, R. T., Ferreira, Ó., & Plomaritis, T. A. (2017). Measuring and modelling overwash hydrodynamics on a barrier island. In T. Aagaard, R. Deigaard, & D. Fuhrman (Eds.), *Proceedings of Coastal Dynamics 2017: Helsingør, Denmark* (pp. 1616-1627). Article 105

Coastal Dynamics 2017
Paper No. 105

MEASURING AND MODELLING OVERWASH HYDRODYNAMICS ON A BARRIER ISLAND

Ana Matias[1], Ana Rita Carrasco[1], Carlos Loureiro[2], Umberto Andriolo[3], Gerd Masselink[4], Martha Guerreiro[5], André Pacheco[1], Robert McCall[6], Óscar Ferreira[1] Theocharis A. Plomaritis[1]

Abstract

Overwash hydrodynamics datasets are mixed in quality and scope, being hard to obtain due to fieldwork experimental difficulties. Aiming to overcome such limitations, this work presents accurate fieldwork data on overwash hydrodynamics, further exploring it to model overwash on a low-lying barrier island. Fieldwork was performed on Barreta Island (Portugal), in December 2013, during neap to spring-tides, when significant wave height reached 2.64 m. During approximately 4 hours, more than 120 shallow overwash events were measured with a video-camera (at 10 Hz), a pressure transducer (at 4 Hz) and a current-meter (at 4 Hz). This high-frequency fieldwork dataset includes runup, overwash number, depth and velocity. Fieldwork data along with information from literature were used to setup XBeach model in non-hydrostatic mode. The baseline model had variable skills over the duration of the overwash episode, performing better during the rising tide than during the falling tide. Model average number of events RMSE (root-mean-square-error) was 7 events each 30 minutes. The baseline model was forced to simulate overwash with different nearshore morphology, grain-size and lagoon water level. An average decrease of about 30% overwash was obtained due to changes in the nearshore morphology, mostly a small vertical growth of the submerged bar. The coarser and finer grain-sizes tests produced an 11% change in overwash, with less overwash on the coarser barrier. Changing lagoon water levels had a reduced effect on overwash hydraulics.

Key words: storm impacts, hydrodynamics, XBeach, runup, nearshore topography, video data.

1. Introduction

Overwash is generally associated with storm conditions with significant wave heights ranging from 3 to 9 m (Matias and Masselink, 2017); however, overwash can also occur during non-storm conditions (Matias *et al.*, 2009). Importantly, the occurrence and magnitude of overwash is dependent not only on the hydrodynamic forcing (wave conditions and water level), but it is also controlled by the site-specific geomorphological context. Field observations are sometimes carried out during overwash episodes, but more commonly are made before and after overwash occurrence. Overwash field investigations principally measure morphological changes induced by overwash; yet, only a limited number of studies also measures overwash hydrodynamics. Moreover, hydrodynamic datasets are mixed in quality and scope, ranging from single hydrodynamic measurements using relatively crude methods (*e.g.* timing floating objects; Bray and Carter, 1992) to more comprehensive and sophisticated approaches (*e.g.* laser scanners; Almeida *et al.,* 2017).

Because measurements are scarce and difficult to obtain, reliable numerical models of simulating overwash are valuable to complement field data (particularly in extreme conditions). In order to manage overwash in areas where it is not desirable, or to reduce the consequences of overwash episodes, a reliable predictive model is required to assess coastal hotspots and to improve coastal defense designs.

The objectives of this work are to model overwash hydrodynamics on a low-lying barrier island where fieldwork measurements were also made and explore it to evaluate the role of several factors influencing

[1]CIMA, Universidade do Algarve, Campus de Gambelas, 8000-Faro, Portugal. ammatias@ualg.pt; azarcos@ualg.pt; ampacheco@ualg.pt; oferreir@ualg.pt; tplomaritis@ualg.pt
[2]Ulster University, BT52 1SA Coleraine, Northern Ireland. c.loureiro@ulster.ac.uk
[3]Universitdade de Lisboa, Campo Grande, C6, 1749-016 Lisbon, Portugal. andriolo.umberto@libero.it
[4]Plymouth University, Plymouth, PL4 8AA, United Kingdom. g.masselink@plymouth.ac.uk
[5]Instituto Hidrográfico, Rua das Trinas, 49, 1249-093 Lisbon, Portugal. Martha.Guerreiro@hidrografico.pt
[6]Deltares, Rotterdamseweg 185, Delft 2629 HD, The Netherlands. Robert.McCall@deltares.nl

overwash hydrodynamics (nearshore morphology, grain-sizes and lagoon water levels).

2. Study area

Fieldwork was performed on the western part of Barreta Island, located in the Ria Formosa, southern Portugal (Figure 1), a multi-inlet island system that extends 55 km along the coast. The field site is located about 1300 m downdrift from Ancão Inlet (Figure 1), which has been migrating towards the fieldwork site since 1997 (Pacheco *et al.*, 2007). The evolution of Ancão Inlet and Barreta Island are strongly related, with island low-volume states associated with sediment starvation due to the updrift trap effect of the inlet (Matias *et al.*, 2009); while high-volume states at Barreta Island related to the arrival of swash bars from the inlet ebb-delta (Vila-Concejo *et al.*, 2006). At the fieldwork site, dune vegetation development on small aeolian mounds was noted since 2001, with remnants still visible close to the backbarrier (Figures 1 and 2); however they are being eroded since 2013 by frequent overwash.

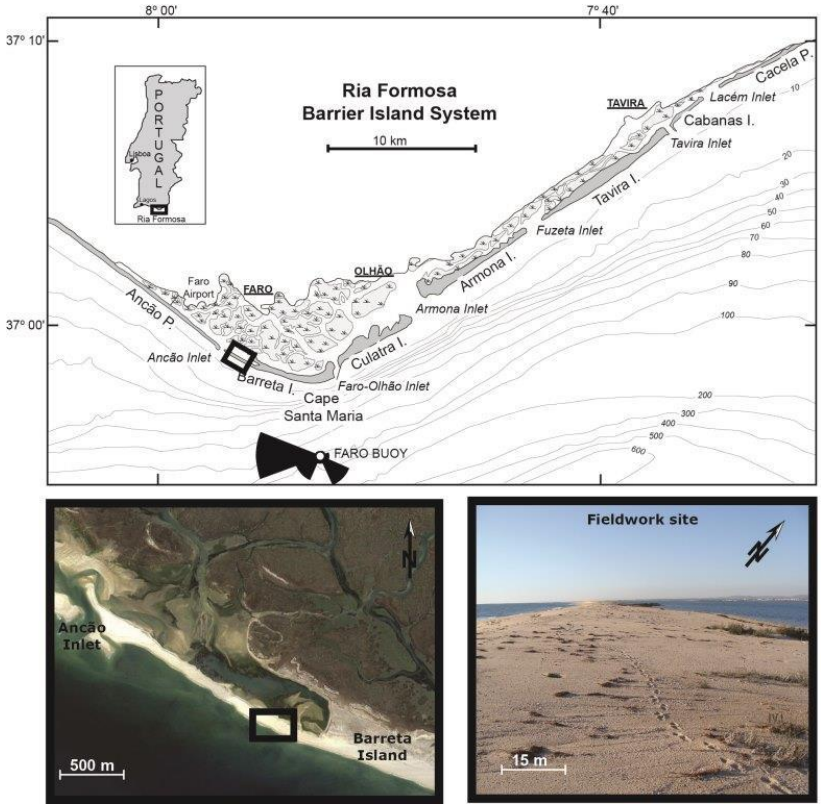

Figure 1. Top: Fieldwork location within the Ria Formosa barrier island system, Algarve, Portugal. Bottom left: Aerial photograph from 2013 showing the study area location on the Western part of Barreta Island, and Ancão Inlet. Bottom right: Ground picture of the study area looking Westwards, with the lagoon and mainland to the right-hand side.

The Ria Formosa barrier system is in a mesotidal regime, with mean tidal range of about 2 m that can reach up to 3.5 m during spring tides. The offshore wave climate is dominated by W-SW waves (71% of occurrences), while short-period SE waves generated by regional winds occur during 23% of the time (Costa *et al.*, 2001). Wave energy is moderate with an average annual significant wave height (H_s) of 1.0 m and average peak period (T_p) of 8.2 s (Costa *et al.*, 2001). Storm events in the region are defined as events with H_s above 3 m (Pessanha and Pires, 1981). The western part of Barreta Island has a Northwest-Southeast orientation, such that it is directly exposed to West-Southwesterly waves, and it is relatively protected from SE waves (Figure 1).

3. Overwash measurements

3.1. Fieldwork campaign

Fieldwork was undertaken during an overwash episode that took place during the 12th and 13th December, 2013. Data collection was undertaken along a cross-shore profile in a low-lying section of the barrier (Figures 1 and 2A), where overwash was expected to occur more frequently.
Offshore waves during the fieldwork campaign were recorded by a directional wave buoy (Datawell Waverider), operated by the Hydrographic Institute of the Portuguese Navy, and located approximately 8 km from the fieldwork site, where water depth reaches 93 m (Figure 1).

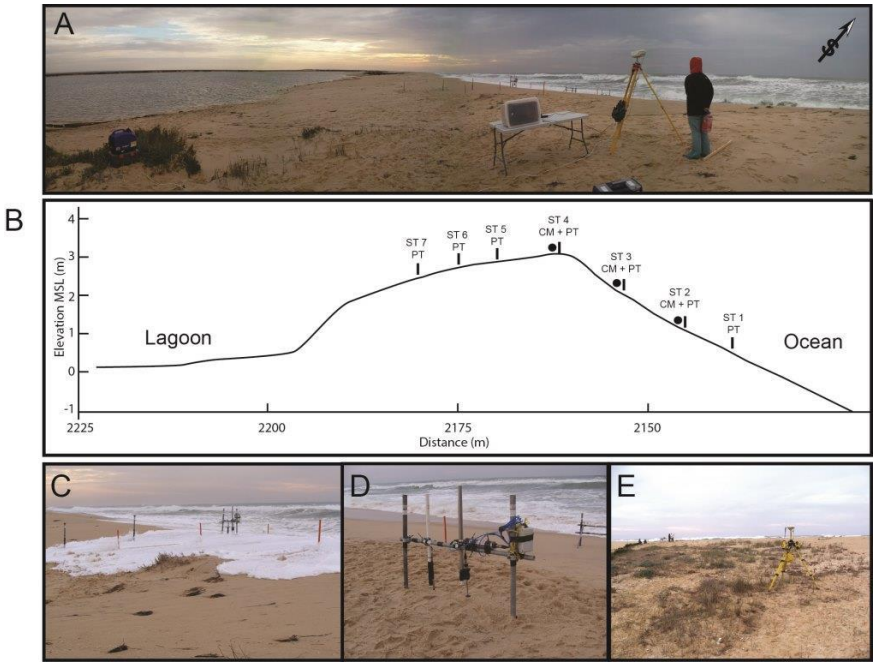

Figure 2. Fieldwork settings. A: Overview of barrier measuring stations and video monitoring system. B: Location of measuring stations across the barrier island. C: Overwash over the barrier crest, with water reaching stations ST 4, ST 5, and ST 6. D: Detail of measuring station ST 4, with the electromagnetic current-meter and data-logger (right hand-side) and the pressure transducer (left-hand side). E: View over the remnants of dune vegetation Westwards of the measuring profile, and the base unit of the DGPS.

The measuring system was composed of seven measuring stations (ST), with sets of instruments (current-meters, CM, and pressure transducers, PT) deployed along a cross-shore profile (Figure 2B). Stations were numbered from the low-tide water level at the beach (ST 1) to the barrier crest (ST 4, Figures 2C and 2D) ending in the backbarrier section, above the lagoon high-water level (ST 7). PTs measuring at 4 Hz were placed in all STs and CMs were placed in ST 2, ST 3 and ST 4. Due to intense erosion during high-tide ST 2 collapsed and ST 3 was damaged. The only operational current meter for the entire duration of the campaign was at ST 4 (located on the barrier crest).
The overwash episode was also monitored by a video camera mounted on a tripod looking sideways at the instrumented cross-shore profile (Figure 2A). The device was composed by an Internet Protocol Vivotek camera, acquiring imagery at 10 Hz, during 4 hours (08:30 to 12:30). The elevation of the camera center of view (COV) was 4.9 m above Mean Sea Level (MSL).
Barrier morphology was measured before and after the overwash episode using an RTK-DGPS (Figure 2E). All instruments and ground-control points for video analysis (red poles in Figure 2C) were also geo-referenced with the RTK-DGPS. Surficial sediment samples were collected at all stations.

3.2. Data processing

Offshore wave conditions measured were obtained for sequential periods of 30 minutes, then transmitted to a land station and quality controlled by the Hydrographic Institute of the Portuguese Navy. In order to obtain the wave conditions in the nearshore area of the study site, the numerical wave propagation model SWAN (Simulating WAves Nearshore; Booij *et al.*, 1999; Ris *et al.*, 1999) was used. SWAN was run in third generation, 2D stationary mode, and implemented using a nested modelling scheme, with model domains composed by a 20 m resolution local grid, nested into the 50 m resolution regional grid. Simulations were initialized in the offshore boundary of the regional grid with the measured 2D spectra from the wave buoy, variable water levels and wind forcing obtained from the nearby Faro Airport (location in Figure 1). SWAN was run in third-generation, two dimensional stationary mode.
Tidal levels in the ocean margin were calculated with an algorithm developed by Pacheco *et al.* (2014); that computes the astronomical constituents with a tidal-analysis toolbox (Pawlowicz *et al.*, 2002) over an hourly time-series for the period 2003-2010 obtained from a tide gauge located on Faro-Olhão Inlet (about 6 km eastwards of the study area, Figure 1). Tidal levels on the lagoon margin were determined using an estimate of the time delay and level shift between oceanic and lagoon tidal levels for this area. The delay and shift were calculated from water level data collected by Popesso *et al.* (2016). Storm surge values during the campaign were obtained from the closest operational tidal gauge located in Huelva, Spain (60 km to the East; Puertos de Estado, online).
Overwash depths were determined using PT data from measuring stations. Since all instruments were synchronized and calibrated for atmospheric pressure in the field, overwash events were identified and isolated using the time tagging provided by the video analysis. The same time tagging was used to obtain overwash event velocity at crest computed from the electromagnetic CM data. Maximum overwash depth and peak velocity were calculated for each overwash event. Overwash timestak images were produced using the pixel array located along the instrumented barrier profile, and considering sampling periods of 10 minutes. Timestack images generated between low tide water level and the barrier crest positions were used to extract wave runup, through coupling manually picked swash events with profile elevation. Timestack images matching the backbarrier profile allowed the identification of each overwash event, here defined as a single passage of water over the barrier crest. On each timestack, the overwash water front was automatically detected by an image processing algorithm based on pixel intensity variation. The average leading edge velocities of each overwash event on the barrier were estimated through the intersection of the detected water time-space line with instruments positions. Runup from each swash event, was visually identified by the edge of each water excursion, on each referenced timestack image.
Cross-shore profiles from the start and end of the overwash episode were used to interpolate the barrier profiles during the overwash, by weighting changes according to the number of overwash events measured during each timeframe. Samples of barrier sediments were analyzed using traditional laboratory dry sieving procedures for unconsolidated clastic sediments. Sieving was done for sediment grain-sizes between 31.5 mm and 0.063 mm. Percentiles D_{10}, D_{50} (median), and D_{90} were determined using GRADISTAT (Blott and Pye, 2001). Sediment porosity was determined volumetrically in the laboratory.

3.3. Fieldwork results

During the fieldwork campaign, which occurred only a couple of days after neap tides, tidal levels reached a maximum of about 0.9 m MSL on the ocean side, between 10:00 and 10:30, whilst lagoon maximum and minimum tidal elevations were 0.17 m and -0.3 m MSL, respectively. Storm surge was very small, between 0.00 m and 0.06 m. Offshore waves had average H_s of 2.5 m, with the highest H_s of 2.64 m recorded at 11:00 (close but not exceeding the storm threshold for this area, 3.0 m). At about 12 m water depth, wave refraction had reduced H_s to 2.0 m – 2.2 m. The main wave direction was from SW, with an offshore incident angle always smaller than 30 degrees.
During most of the overwash episode wave spectra were relatively broad, slightly narrower at the beginning (8:30, Figure 3). The highest wave energy peak was associated with wave frequencies around 0.09 Hz, with a second mode around 0.11 Hz (Figure 3). At water depths of 15 to 17 m energy in the infragravity band was limited; rather a tail towards the high-frequency waves was noticed. Although

several and variable peaks in wave spectra were recorded offshore, two main sets of waves could be identified. By fitting one or two JONSWAP type of spectrum to the measured curves, the wave sets characteristics were obtained: waves with average H_s of 2.0 m and T_p of 11.3 s, and waves with average H_s of 1.3 m and T_p of 8.8 s.

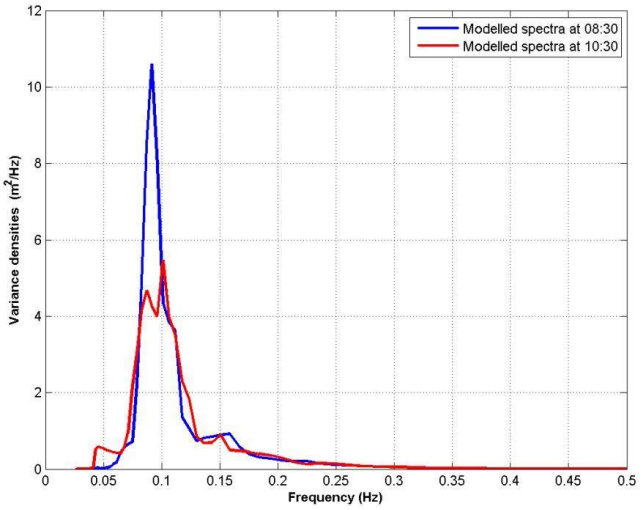

Figure 3. Examples of modeled nearshore wave spectra, at 15 m water depth, for the time-steps 08:30 and 10:30, of 12/12/2013.

Over more than 4 hours, *circa* 120 overwash events occurred over the barrier crest of the selected profile. About 70% of these events occurred between 10:30 and 12:30 (Figure 4). Most overwash events had limited onshore intrusion (< 2 m) on the top of the barrier; yet, some events reached the backbarrier lagoon. Peak overwash flow velocity was generally between 1 - 3 ms^{-1}, though maximum velocities reached values close to 6 ms^{-1}. Overwash flow was very shallow (Figure 4), with mean depth of 6.7 cm. These characteristics are typical of overwash flows, which generally are supercritical (according to data compiled by Matias and Masselink, 2017). Usually, the larger overwash events had concomitant deeper and faster flows, with longer durations and larger intrusion distances. Despite the reduction in number of events at the start and end of the overwash episode and variable peak velocities, the overwash depth was relatively constant (Figure 4).

During the overwash episode, the beach face was eroded and sand accumulated on the barrier top and across the barrier (Figure 5). Observed changes indicate that the volume of barrier erosion was greater than the volume of overwash induced deposition. The net sediment balance is -13.7 m^3m^{-1}, with only about 1.8 m^3m^{-1} of overwash deposition on the barrier. This result may have several explanations, such as a longshore component of sediment transport that was not measured; or there was an offshore sediment transport to areas below the topographic survey undertaken during fieldwork. Topography at the end of the overwash episode was only surveyed up to -1 m MSL on the ocean margin; below this depth, another former nearshore survey was used. The nearshore area, between -1 m and -3.5 m MSL (Figure 5) typically exhibits a bar that changes in morphology and elevation through time, with an average slope of 0.01, and average D_{50} of 0.36 mm (computed with data published in Rosa et al., 2013). Seaward of the bar, the profile is planar with a gentler slope of 0.008, and an average D_{50} of 0.43 mm. The beach face is steep (average slope of 0.1), with average beach D_{50} of 0.61 mm. The backbarrier surface facing the lagoon has variable slopes, and exhibits a coarsening grain-size and a poorer sorting due to the presence of overwash debris lines. Barrier porosity is mostly around 0.3; with a maximum of 0.36 close to ST7 (location on Figure 2).

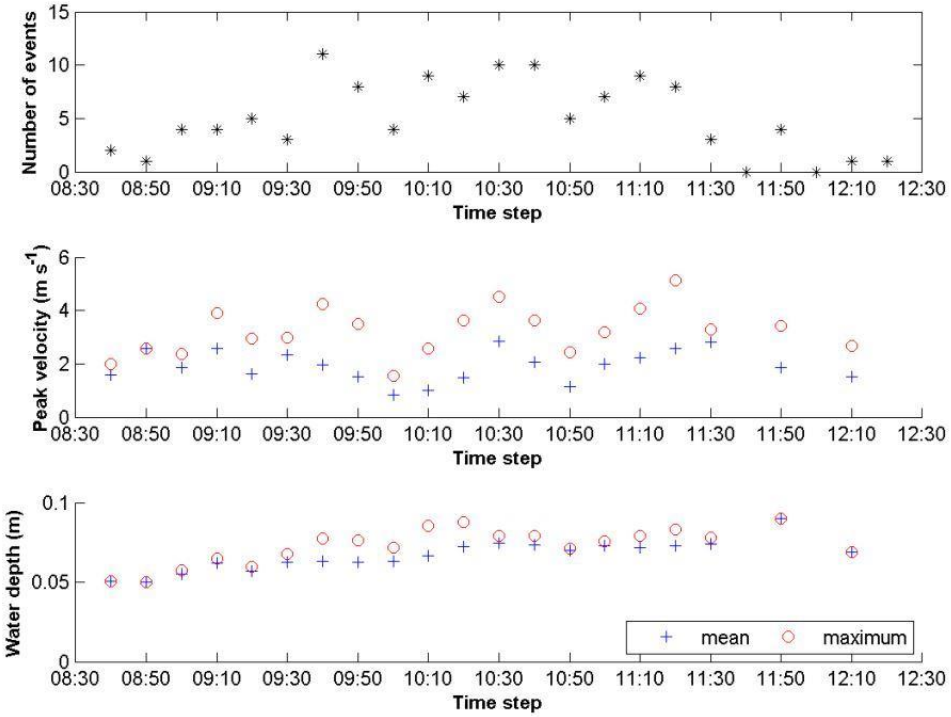

Figure 4. Overwash events average properties during the overwash episode, measured in ST 4 (see Figure 2 for location).

4. Hydrodynamic modelling

4.1. Model set-up

This study used the one-dimensional approach of XBeach model developed by Roelvink et al. (2009), in non-hydrostatic mode. The model was run without the computation of morphology. Model setup consisted of three stages: definition of boundary forcings, generation of the model grid and model calibration. The boundary forcing conditions were parameterized using fieldwork measurements when available (barrier profile (Figure 5), wave spectra (Figure 3), ocean and lagoon water levels, and median grain-size), whilst other parameters were kept with default values (*e.g.* bed friction). The hydraulic conductivity (k) was computed with Hazen's equation, using measured D_{10}. The generated grid is non-equidistant, with a minimum grid size of 0.1 m and a maximum grid size of 3 m, observing the condition of a minimum of 50 points per wavelength. XBeach calibration was carried out by tuning three parameters:

1. Offshore boundary - It was decided by balancing two opposite criteria: (i) it should be located in deep water, considering the longest waves; and (ii) it should be located in water shallow enough to account for most of wave refraction. Considering the wave conditions measured during the overwash episode and a ratio between wave group velocity and phase velocity < 0.85, a boundary deeper than 17 m would be preferable. However, as waves at this depth were not yet shore-normal (12^o - 26^o) and refraction cannot be accounted for in a 1D model, the offshore boundary was set in an intermediate location, at -15 m MSL.
2. Spin-up duration - XBeach in non-hydrostatic mode is a phase-resolving model; therefore, at the start of each run waves propagating across the nearshore do not reach the barrier (the domain exceeds 2000 m). Runs were made with an initial time (the 'spin-up') of 10, 20 and 30 minutes durations. It was concluded that a spin-up of 10 minutes provided good results whilst maintaining a reasonable computational effort.
3. Number of replicates - Since a wave-spectrum is a statistical quantity obtained over 30-minutes, a number of model outputs can be obtained with the same setup. A power analysis was made to estimate the number of replicates needed to allow accurate and reliable statistical judgments. A mean number of 160 overwash events and a standard deviation of 10 were used, based on an average obtained of prospective 30

replicates made initially. An effect size of 10% and a power of 95% were decided based on the literature (*e.g.* McDonald, 2014), and assured a very high chance of observing an effect that is real. The obtained number of replicates was 6.

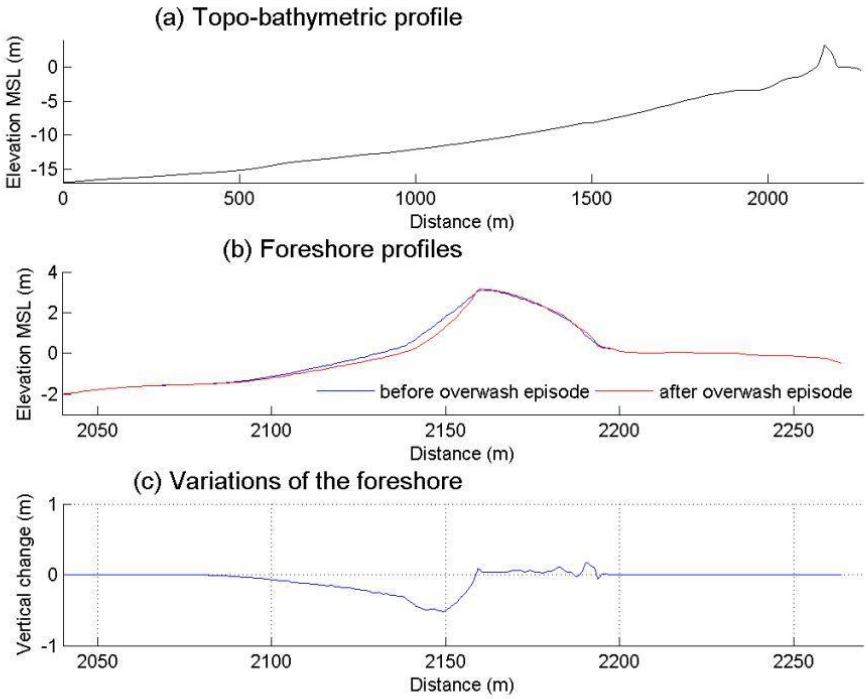

Figure 5. A: Topo-bathymetric profile of the study area. B: Topographic profiles of the barrier before and after the overwash episode. C: Morphologic variation of the barrier during the overwash episode.

Due to the high resolution of the computational grid, the overwash episode was divided into 9 time steps of 30 minutes (with 10 minutes spin-up), from 08:30 to 12:30. The output time-step was set at 4 Hz, matching the sampling grid of the instruments.

4.2. Model performance

The model performance and evaluation of its usefulness as a predictive tool was assessed using standard metrics of performance, particularly bias, root-mean-square error (RMSE), and scatter index (SCI), as described e.g. in McCall *et al.* (2014). The baseline model performance metrics are presented in Table 1.

Table 1. Performance metrics of baseline model according to average number, depth and velocity of overwash events.

	number	Depth (m)	Velocity (ms^{-1})
Bias	5	0.02	0.43
RMSE	7	0.02	0.61
SCI	0.27	0.30	0.28

It can be observed that the model overestimates overwash number; for each time-step an average of 5 extra overwash events are produced by the model, which represents about 25 % extra events. The model performance change throughout the event; during the rising tide the baseline model under or over predict

by only 2 to 4 events, while during the falling tide the baseline model over predicts overwash by 4 to 14 events.
Overwash depth and velocity are also overestimated by about 20%; however these values are very small (0.02 m and 0.4 ms^{-1}), within the error margin of the measurements under the demanding fieldwork conditions. The SCI for the number, depth and velocity of overwash events is consistently low to moderate (circa 0.3).
The comparison between the fieldwork runup statistics and the modelled runup statistics is also an indicator of the model performance. Due to the high number of overwash events, the R2 (2% exceedance runup) is not an adequate indicator, since R2 basically reflects the barrier crest elevation. Instead, the Rsig (significant runup, *i.e.*, the average of the top third of runup values) was calculated. The average difference between the field Rsig and the model Rsig each 10 minutes is 0.2 m, with the model overestimating fieldwork. Because overwash flows are so shallow, a 0.2 m difference in significant runup allows an extra 25% of overwash events over the crest. Even though for the measured conditions, the Barreta baseline overwash model overestimates runup and overwash in the order of 20 to 25%, it can be considered as a fairly good tool from a conservative approach perspective.

4.3. Model analysis

The Barreta baseline overwash model was explored to analyze the relative importance of several factors in the occurrence of overwash, namely: (1) the nearshore morphology; (2) the barrier grain-size; and (3) the lagoon water levels. For the analysis of these factors, the Barreta baseline overwash model was changed in only one parameter at a time, keeping the remaining unaltered. Each modified model was also replicated 6 times, therefore presented results are ensemble means. The output variables (runup, overwash number, depth, velocity and discharge) were compared with the baseline model, to try and understand their importance in overwash processes.
The nearshore morphology is known to change significantly in the study area (e.g. Vila-Concejo *et al.*, 2006), as a consequence of the migration of swash bars from the updrift Ancão Inlet. Several nearshore morphological configurations of the study area were available (data from Matias *et al.*, 2014) and the one that deviates most from the configuration during the overwash episode was selected. It was surveyed in June 2012, when the nearshore bar crest was higher in comparison to the configuration used for the baseline model (February 2013). The new bathymetric grid was built with the same resolution and dimensions of the baseline model, and the same oceanographic forcing was superimposed, which implied new SWAN runs over the new bathymetric grid. Results are summarized in Figure 6.
Significant differences are observed between the baseline model and the nearshore model (Figure 6). There is a noticeable reduction in the number of overwash events with the nearshore model, from 160 to 105 events, particularly evident during high-tide when a reduction of more than 40% is observed. The average overwash depth and velocity also changed, but the reduction is very small (-2 mm average depth and -0.06 ms^{-1} overwash velocity). Overall, discharge for the baseline model was 45 $m^3m^{-1}s^{-1}$, while for the nearshore model was 27 $m^3m^{-1}s^{-1}$, which corresponds to 40% reduction. The runup statistics differences show a reduction in runup on the nearshore model (Rsig decreased 0.22 m in relation to baseline model). Average Rsig of the nearshore model is, however, closer to fieldwork then the baseline model.
Previous studies in the area highlighted some grain-size variability of the barrier, both in the beach face and the barrier washovers. Data published in Matias *et al.* (2009) were used to obtain a measure of the likely grain-size variability and hence set the finer and coarser grain-size models. The finer grain-size model was set with D_{50} = 0.47 mm, which implied a change of k to 0.001 ms^{-1} associated with a D_{10} of 0.32 mm. The coarser grain-size model was set with D_{50} = 0.89 mm (D_{10} = 0.393 mm; k=0.0015 ms^{-1}).

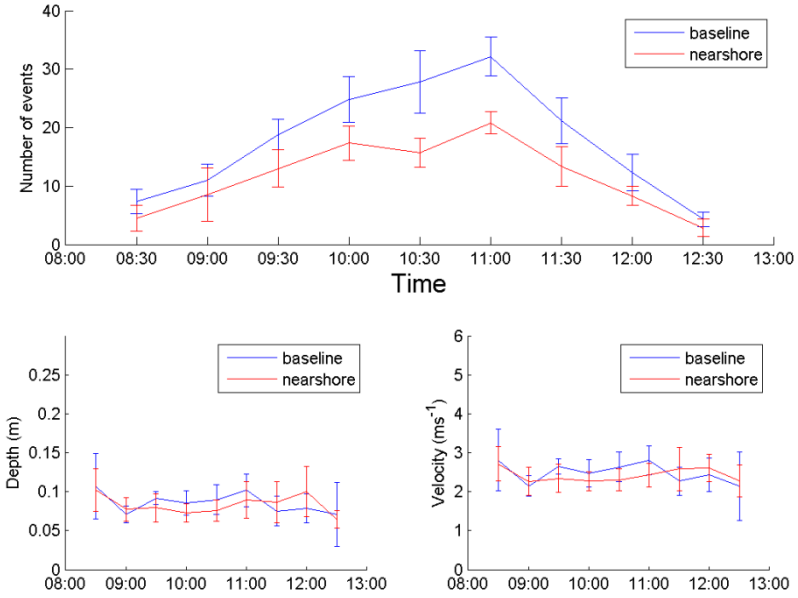

Figure 6. Overwash event number and hydrodynamic variables from the baseline model and from the nearshore model.

The comparison between the baseline model and the finer and coarser grain-size models showed that the finer grain-size model was the one producing more overwash, while the coarse grain-size model led to a decrease in overwash (Figure 7). The change in overwash events was significant, from 160 in the baseline model to 178 in the finer model and 142 in the coarser model. Again, the changes were particularly evident in the number of overwash events comparing to the other hydrodynamic variables (depth and velocity changes were always smaller than 1 mm and 0.03 ms^{-1}, respectively). Overall discharges reduced 8% in the coarser and increased 7% in the finer grain-size models in relation to the baseline model. Rsig of coarser grain-size model decreased 0.03 m in relation to baseline, while average Rsig of finer grain-size model increased in 0.01 m.

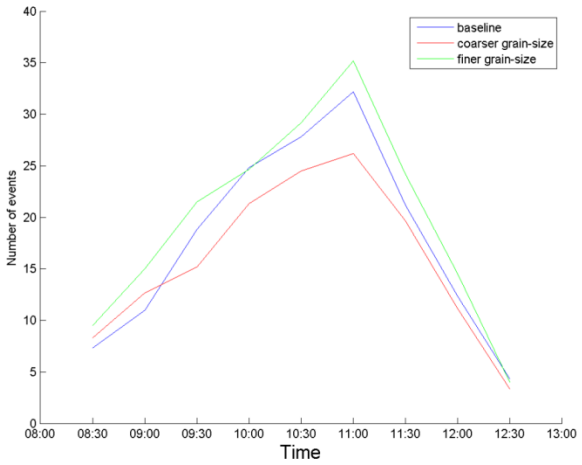

Figure 7. Average number of events for each time-step of the baseline model and the different grain-sizes models.

To test the importance of lagoon levels in overwash occurrence, the model was set with the maximum ocean and lagoon water level distances for the fieldwork campaign. The baseline model hydraulic gradient

was always negative (between -0.0054 and -0.0132, towards the lagoon), because the lagoon levels were consistently lower. To test other situations, a high lagoon model was set up in which the lagoon level was at z=0.88, whilst for the low lagoon model the water level was at z=-0.28. These changes generated model simulations with the highest hydraulic gradient (0.007) for the high lagoon model during oceanic low-tide; and a minimum hydraulic gradient (-0.01) for the low lagoon model, during oceanic high-tide. Even if the lagoon water level could be lowered, the hydraulic gradients would not change significantly because of the morphology of the backbarrier lagoon (Figure 2A). As the water level reaches the lagoon low-tide flat, a small change in elevation implies a great increase in horizontal distance, thus lowering the gradient. The results of the high lagoon, low lagoon and the baseline models present small average variations. The greater average variation in overwash number between the lagoon models and the baseline model was 2 events/time-step, which is not significant. The contrasting high lagoon and low lagoon models deviate very little from each other (0 - 15%).

5. Discussion and conclusions

Data from an overwash episode are presented in this study. The overwash episode occurred during mid-tide to high tide (maximum oceanic tidal elevation of 0.9 m above MSL), with bimodal waves that resulted from the combination of swell waves with variable periods and heights. During this moderate wave energy event, overwash was not prevalent along most of the Ria Formosa barrier islands as wave runup was consistently lower than dune elevation. On the contrary, the fieldwork study site (a low-lying barrier stretch) experienced more than 100 overwash events.

Field observations showed that morphological changes were relatively small. Sediments were eroded away from the sub-aerial beach, and only partially deposited on the barrier top, while a portion was likely transported to lower depths. Similar evolution was also recorded in recent high-resolution 2D laser scanner measurements of overwash by Almeida *et al.* (2017).

Barreta Island most common overwash flow was very shallow (mean depth of 0.067 m) and relatively fast, with peak velocities in the range 1 - 3 ms^{-1}. Such supercritical flows compare well with typical fieldwork and laboratory measurements that can be found in Matias and Masselink (2017).

Fieldwork data and published data from overwash on Barreta Island were used to setup a baseline model of overwash hydrodynamics using Xbeach in non-hydrostatic mode. The baseline model performance metrics was assessed by comparison with fieldwork by mean of bias, RMSE and SCI. The baseline model has a positive bias, therefore overestimating the number of overwash events, and an overall RMSE = 7. These differences between predictions and observations may be related to several factors. Morphologic changes occurring during overwash in the submerged, non-monitored part of the beach profile can influence subsequent overwash hydrodynamics. Moreover, the baseline model was set with the most recent bathymetry in the area, measured in February 2013, 10 months before the overwash fieldwork. Additionally, there is a lack of data from waves in the nearshore and swash areas. Nearshore wave transformation was simulated with the model SWAN and there is no comparison with fieldwork results because instruments located in this area during high tide (ST 1 to ST3) fall down or failed. Considering all limitations in fieldwork measurements and possible sources of error, it was considered that the baseline model still provided a reasonable agreement with field data. Further encouraging results of XBeach implementation for overwash investigation were also obtained by McCall *et al.* (2010) on a sandy beach, Almeida *et al.* (2017) on a gravel beach and Masselink *et al.* (2014) in laboratory experiments.

The importance of nearshore bathymetry for overwash processes on Barreta Island was evaluated by setting the nearshore model, which was identical to the baseline model except for the bathymetry that evidenced more changes in relation to the baseline configuration. Results indicate an average difference of about 30% of overwash events, with the nearshore model inhibiting overwash. Based on results, the nearshore bar is considered to be an important factor because nearshore morphological variability in this area is significant, given the detachment and longshore migration of swash bars from the updrift Ancão Inlet. The role of beach morphology was also found to be crucial in modelling wave overtopping with Xbeach by Phillips *et al.* (2017), in an area of North Wales, U.K., where coastal flooding is a hazard to populations.

Although the main sedimentary source to the study area is relatively constant (longshore drift and inlet associated dynamics), some sand grain-size variability was detected in the area (Matias *et al.*, 2009). The

impact on model results arising from realistic grain-size changes was tested by running the coarser and finer grain-size models. The tested grain-sizes are all within sand grain-size range, and are basically composed of medium to coarse sand. On average the coarser grain-size model promoted less overwash (-11 % overwash events number and -8% discharge), than the baseline model. An intensification of overwash was recorded with the finer grain-size model. This means that there may be small to moderate overwash hydrodynamic changes in the study area induced solely by its natural grain-size variability.
The impact of lagoon water levels on overwash hydrodynamics, and implicitly the groundwater gradient between the ocean and lagoon water bodies, was also tested. The lagoon water levels were set to maximum and minimum elevations concomitant with opposite ocean tide levels. Modelling results show small changes in hydrodynamic quantities. Even with unrealistic hydraulic gradient changes, the model still predicts less than 10% changes in overwash hydraulics. Assuming the model reproduces correctly the groundwater flows, results from this study suggest that the lagoon water elevation exerts limited influence in overwash, at least when compared with the impacts of nearshore morphology and grain-size. Almeida *et al.* (2017) implementation of Xbeach model on a gravel barrier also found that groundwater gradients do not produce a significant difference in modelled overwash discharges.
As a general conclusion, the baseline model developed here is able to provide a first attempt to predict the occurrence and hydrodynamics of overwash in the study area. Nevertheless, more work is necessary to validate the model with different wave, tide and morphological characteristics. The tested models implementations (nearshore model and grain-size models) have demonstrated that to assure model reliability a continuous monitoring of the topography, bathymetry and grain-size is mandatory.

Acknowledgements

This study was supported by RUSH project, PTDC/CTE-GIX/116814/2010 and EVREST project, PTDC/MAR-EST/1031/2014, financed by FCT, Portugal. A. Matias and A. Pacheco were supported by Investigator Programme, IF/00354/2012 and IF/00286/2014, respectively, financed by FCT, Portugal. A.R. Carrasco was supported by SFRH/BPD/88485/2012. T. Plomaritis is funded by the EU FP7 research project RISC-KIT (ref. RISC-KIT-GA-2013-603458).

References

Almeida, L.P., Masselink, G., McCall, R., Russell, P., 2017. Storm overwash of a gravel barrier: field measurements and XBeach-G modelling. *Coastal Engineering*, 120: 22-35.

Blott, S.J. and Pye, K., 2001. GRADISTAT: a grain size distribution and statistics package for the analysis of unconsolidated sediments. *Earth Surface Processes and Landforms*, 26: 1237-1248 technical communication.

Booij, N., Ris, R.C., Holthuijsen, L.H., 1999, A third-generation wave model for coastal regions: 1. Model description and validation. *Journal of Geophysical Research*, C4, 104: 7649-7666.

Bray, T.F. and Carter, C.H. 1992. Physical processes and sedimentary record of a modern, transgressive, lacustrine barrier island. *Marine Geology*, 105, 155-168.

Costa, M., Silva, R., Vitorino, J., 2001. Contribuição para o estudo do clima de agitação marítima na costa portuguesa. Proceedings of *2as Jornadas Portuguesas de Engenharia Costeira e Portuária*, PIANC, Sines, Portugal.

Masselink, G., McCall, R., Poate, T., van Geer, P., 2014. Modelling storm response on gravel beaches using XBeach-G. *Maritime Engineering*, 167: 173-191.

Matias, A. and Masselink, G., 2017. Overwash processes: lessons from fieldwork and laboratory experiments. In: *Coastal Storms: Processes and Impacts*. (Ed.) Paolo Ciavola and Giovanni Coco, John Wiley & Sons Ltd., pp. 175-194.

Matias, A., Vila-Concejo, A., Ferreira, Ó., Morris, B., Dias, J.A., 2009. Sediment dynamics of barriers with frequent overwash. *Journal of Coastal Research*, 25 (3): 768–780.

Matias, A., Carrasco, A.R., Loureiro, C., Almeida, S., Ferreira, Ó., 2014. Nearshore and foreshore influence on overwash of a barrier Island. *Journal of Coastal Research*, SI 70, 675-680.

McCall, R.T., de Vries, J.S.M., Plant, N.G., van Dongeren, A.R., Roelvink, J.A., Thompson, D.M., Reniers, A.J., 2010. Two-dimensional time dependent hurricane overwash and erosion modelling at Santa Rosa Island. *Coastal Engineering*, 57: 668-683.

McCall, R.T., Masselink, G., Poate, T.G., Roelvink, J.A., Almeida, L.P., Davidson, M., Russell, P.E., 2014. Modelling storm hydrodynamics on gravel beaches with XBeach-G. *Coastal Engineering*, 91: 231-250.

McDonald, J.H. 2014. Handbook of Biological Statistics (3rd ed.). Sparky House Publishing, Baltimore, Maryland.

Pacheco, A., Vila-Concejo, A., Ferreira, Ó., Dias, J.A., 2007. Present hydrodynamics of Ancão Inlet, 10 years after its

relocation. Proceedings of *Coastal Sediments '07*, ASCE, New Orleans (USA), pp. 1557–1570.

Pacheco, A., Ferreira, Ó., Carballo, R., Iglesias, G., 2014. Evaluation of the production of tidal stream energy in na inlet channel by coupling field data and numerical modelling. *Energy*, 71: 104-117.

Pawlowicz, R., Beardsley, B., Lentz, S., 2002. Classical tidal harmonic analysis including error estimates in MATLAB using T_TIDE. *Computers & Geosciences*, 28: 929-937.

Pessanha, L.E. and Pires, H.O., 1981. *Elementos sobre o clima de agitação marítima na costa sul do Algarve*. Report of Instituto Nacional de Meteorologia e Geofisica. 66 pp. (in Portuguese).

Phillips, B.T., Brown, J.M., Bidlot, J.R., Plater, A.J., 2017. Role of beach morphology in wave overtopping hazard assessment. *Journal of Marine Science and Engineering*, 5(1),1.

Popesso C., Pacheco A., Fontolan, G., Ferreira Ó., 2016. Evolution of a relocated inlet migrating naturally along an open coast. *Journal of Coastal Research,* SI (75): 233-237.

Puertos del Estado (online). Historical data of sea level for Huelva Tidal Gauge. Ministerio de Fomento. Gobierno de España. Available at: http://www.puertos.es/en-us/oceanografia/Pages/portus.aspx

Ris, R.C., Holthuijsen, L.H., Booij, N., 1999. A third-generation wave model for coastal regions: 2. Verification. *Journal of Geophysical Research*, 104, C4, 7667-7681.

Roelvink, D., Reniers, A., van Dongeren, A., de Vries, J., McCall, R., Lescinski, J., 2009. Modeling storm impacts on beaches, dunes and barrier islands. *Coastal Engineering*, 56: 1133–1152.

Rosa, F., Rufino, M., Ferreira, Ó., Matias, A., Brito, A.C., Gaspar, M., 2013. The influence of coastal processes on inner shelf sediment distribution: The Eastern Algarve Shelf (Southern Portugal). Geologica Acta, 11, 59-73.

Vila-Concejo, A., Matias, A., Ferreira, Ó., Dias, J.A., 2006. Inlet sediment bypassing to a downdrift washover plain. *Journal of Coastal Research*, SI 39: 401–405.